

2014-8

A Soft Condensed Matter Approach Towards Mathematical Modelling of Mass Transport and Swelling in Food Grains

Michael Chapwanya
University of Pretoria

N. Misra
Technological University Dublin, misra.nrusimhanath@tudublin.ie

Follow this and additional works at: <https://arrow.tudublin.ie/schfsehart>



Part of the [Complex Fluids Commons](#), [Condensed Matter Physics Commons](#), [Food Processing Commons](#), [Partial Differential Equations Commons](#), [Polymer and Organic Materials Commons](#), [Polymer Science Commons](#), [Thermodynamics Commons](#), and the [Transport Phenomena Commons](#)

Recommended Citation

M. Chapwanya, N.N. Misra (2015) A soft condensed matter approach towards mathematical modelling of mass transport and swelling in food grains, *Journal of Food Engineering*, 145:37-44. <http://dx.doi.org/10.1016/j.jfoodeng.2014.08.010>

This Article is brought to you for free and open access by the School of Food Science and Environmental Health at ARROW@TU Dublin. It has been accepted for inclusion in Articles by an authorized administrator of ARROW@TU Dublin. For more information, please contact arrow.admin@tudublin.ie, aisling.coyne@tudublin.ie, vera.kilshaw@tudublin.ie.

A soft condensed matter approach towards mathematical modelling of mass transport and swelling in food grains

M. Chapwanya^a, N.N. Misra^{b,*}

^a*Department of Mathematics & Applied Mathematics, University of Pretoria, Pretoria 0002, South Africa*

^b*School of Food Science & Environmental Health, Dublin Institute of Technology, Dublin 1, Ireland.*

Abstract

Soft condensed matter (SCM) physics has recently gained importance for a large class of engineering materials. The treatment of food materials from a soft matter perspective, however, is only at the surface and is gaining importance for understanding the complex phenomena and structure of foods. In this work, we present a theoretical treatment of navy beans from a SCM perspective to describe the hydration kinetics. We solve the transport equations within a porous matrix and employ the Flory-Huggin's equation for polymer-solvent mixture to balance the osmotic pressure. The swelling of the legume seed is modelled as a moving boundary with an explicit transient equation. The model exhibits a good agreement with the experimental observations and is capable of explaining the stages of hydration. Sensitivity analysis indicated that the degree of hydration is dependent on the bean size and is also sensitive to the selection of the intrinsic permeability of the bean.

Keywords: Soft Condensed Matter, Hydration, Swelling, Flory-Huggins, Mass Transfer, Navy Bean

1. Introduction

Soaking and hydration of legumes and cereals is an important unit operation in the grain processing industries. For example, legumes such as navy bean and kidney bean are often hydrated prior to canning operations. Hydration of beans decreases the cooking time,

*Corresponding author

Email address: misra.nrusimhanath@dit.ie (N.N. Misra)

13 minimizes losses and improves the nutritional quality and protein digestibility of the cooked
14 product (Wang et al, 1979; Abd El-Hady and Habiba, 2003). The problem of mass trans-
15 fer during hydration of food grains has been treated both experimentally and theoretically,
16 and in studies combining both approaches (Zanella-Díaz et al, 2014; Cozzolino et al, 2013;
17 Ghafoor et al, 2014; Nicolin et al, 2012; Bello et al, 2010; Mohoric et al, 2004; Peleg, 1988;
18 Hsu, 1983). Most of the mathematical descriptions reported in literature are either data
19 driven regression models describing hydration kinetics or are based on simple fickian diffu-
20 sion. Diffusion in many legumes (and cereals) cannot be described adequately by a simple
21 concentration dependent form of Fick's diffusion equation, especially when these undergo
22 swelling (or large deformation in geometry). Such conventional approaches fail to capture
23 the finer details of food structure and their dynamics. Because of the complexity of food sys-
24 tems, interdisciplinary scientific approaches are needed to enable demanding developments
25 (Ubbink and Mezzenga, 2006; Ubbink et al, 2008).

26 Soft matter physics focusing on description of an increasingly important class of materials
27 that encompasses polymers, liquid crystals, complex fluids, organic-inorganic hybrids, foams,
28 gels and the whole area of colloidal science is a contemporary area of research with several
29 opportunities. Soft matter science plays an important role in a wide variety of processes and
30 applications, examples of which include polymer swelling, phase separation, transport and
31 delivery of drugs etc. The principles of soft matter physics are equally applicable to many
32 food systems. Mezzenga et al (2005) reviewed the nature of foods from a perspective of soft
33 condensed matter physics. The details of structural changes at various scales in food systems
34 often needs experimental and/or theoretical tools of soft matter physics, which are not fully
35 adapted to food systems (Mezzenga, 2007; Mezzenga et al, 2005). An exposition of the
36 potential of soft matter physics for explaining the complex food processes and structuring at
37 various scales is also provided in van der Sman and van der Goot (2009) and van der Sman
38 (2012).

39 About 60 years ago, Flory and Huggins independently proposed the lattice model to
40 treat the mixing enthalpy and entropy of polymers in a very straightforward way (Huggins,
41 1942a,b; Flory, 1953). Although many other models have been developed to describe the

42 thermodynamics of polymer systems, the original Flory-Huggins lattice theory always give
43 a very clear and straightforward physical picture (Han and Akcasu, 2011). However, it is
44 worthwhile noting that the Flory-Huggins theory also is based on some assumptions that
45 are often not valid. This includes the assumption that volume changes are not incurred
46 upon mixing the polymer and solvent. It is also supposed that the polymer chain can be
47 modelled on a lattice, which excludes contributions to the entropy from chain flexibility,
48 and specific solvent-polymer interactions are ruled-out (Hamley, 2007). In an early work,
49 van der Sman (2007) deduced an excellent modelling framework based on soft condensed
50 matter perspective to explain the heat and mass transport during cooking of meat. This
51 was based on the Flory-Rehner theory for pressure driven mass-transport in swelling or
52 shrinking gels.

53 The model that we present in this paper is an attempt at advancing the basis of the
54 theoretical modeling of mass transport during hydration of porous foods with a soft matter
55 perspective. The model described herein shares an integrated approach between the sta-
56 tistical thermodynamics based Flory-Huggins theory and the continuum mechanics of fluid
57 transport in porous media. We take an example case of hydration of navy bean, which is
58 modelled as a saturated porous media undergoing large deformation by swelling. We are
59 including a comparison of the simulation results with experimental data as model valida-
60 tion and an illustration of the model application, while also reporting on the sensitivity of
61 the model to selected parameters. By means of the latter, we attempt to both analyse the
62 influence of the natural variability in food properties on model predictions as well as gauge
63 the sensitivity of the model to potential errors in parameter estimation.

64 **2. Problem description**

65 Figure 1, provides a summary of the geometric domain of the bean under consideration.
66 The geometry of the navy bean can be described as a porous scalene ellipsoid, which is
67 capable of undergoing global deformation. For the present study, we also assume that the
68 pores are ideally filled with water which simplifies the problem to a saturated porous media
69 case. We assume that the complex structural elements of navy bean, mainly proteins and

70 carbohydrates can be approximated as ideal polymers. When applying principles of soft
71 condensed matter physics to foods, it may be noted that polysaccharides and proteins are
72 to foods what polymers are to soft condensed matter (Mezzenga et al, 2005). Notably, navy
73 beans are by large chemically comprised of starch (50 - 60%), protein (20 - 38 %) and
74 fibre ($\sim 18\%$) (Kereliuk and Kozub, 1995; Berg et al, 2012). This gives sufficient reason to
75 justify our soft condensed matter analogy for navy beans. To formulate a feasible model, we
76 also assume that the outer pericarp/skin is very thin and has no influence on the moisture
77 transport.

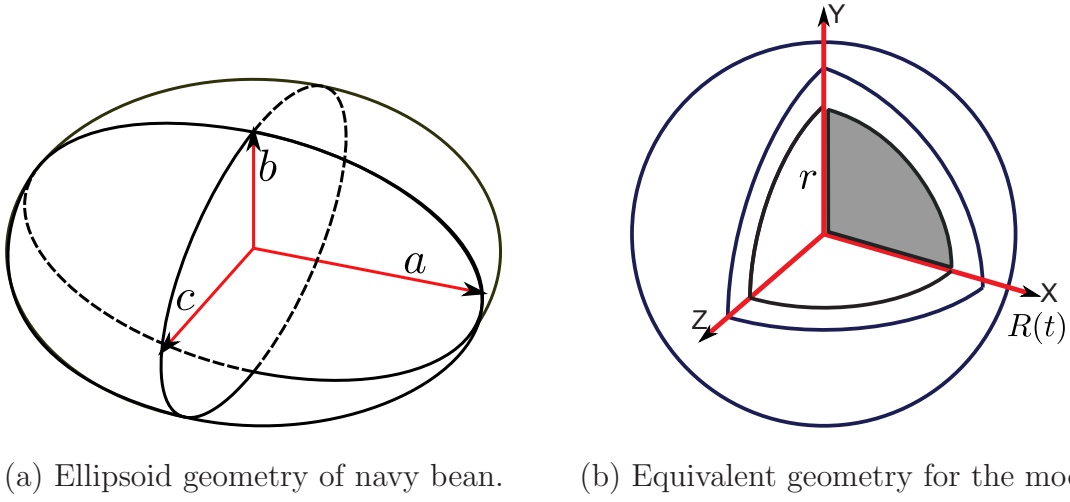


Figure 1: Schematic illustration of (a) the ellipsoid geometry of a navy bean grain and (b) the equivalent sphere concept with model boundaries.

78 We now simplify the problem geometry, by assuming that bean is spherical in shape and
79 the swelling gives an evolving radius, $R(t)$ which varies with time, t . While assuming a
80 spherical geometry for simplicity, we account for the deviations from the ellipsoid solid by
81 calculating the radius of the sphere whose volume is equal to that of the scalene ellipsoid
82 (Figure 1 (b)). The following equation was employed for calculating the equivalent radius,
83 r [mm] (see Figure 1 (a) for notation)-

$$r = \left(\frac{G_m + S_m + A_m}{6} \right) \quad (1)$$

84 Herein, $G_m = 2(abc)^{\frac{1}{3}}$, $A_m = \left(\frac{2a + 2b + 2c}{3}\right)$, and $S_m = \left(\frac{4ab + 4bc + 4ca}{3}\right)^{\frac{1}{3}}$ are the
85 geometric mean diameter, arithmetic mean diameter, and square mean diameter, respec-
86 tively (Mohsenin, 1986). In accordance with Ghafoor et al (2014), we take the temperature
87 to be constant (16 °C) throughout the duration of soaking and therefore, temperatures ca-
88 pable of causing gelatinisation are not encountered. Finally, we define the volume fraction
89 of the solids in the bean to be ϕ , and to satisfy the criteria of saturation, we have $(1 - \phi)$
90 as the volume fraction of the liquid water.

91 3. Mathematical model

92 In this section a mathematical model based on the Flory-Huggins theory for hydration
93 of Navy bean is presented. Part of the modeling approach has been presented elsewhere
94 in the literature in the context of biofilms (Winstanley et al, 2011). For completeness, we
95 summarize the equations here. Mass conservation of the polymer is given by

$$(\rho_s \phi)_t + \nabla \cdot [\rho_s \phi \mathbf{v}] = 0, \quad (2)$$

96 where ρ_s [Kg m⁻³] is the averaged phase density and \mathbf{v} [ms⁻¹] is the protein velocity.
97 Similarly, conservation of the liquid is given by

$$(\rho[1 - \phi])_t + \nabla \cdot [\rho(1 - \phi)\mathbf{w}] = 0, \quad (3)$$

98 where ρ [Kg m⁻³] is the averaged water density and \mathbf{w} [ms⁻¹] is the water velocity.

99 The bean is assumed to be a porous structure, hence the momentum equations as given
100 by Darcy's law holds. We relate the liquid velocity to the liquid pressure, p [Pa], via

$$-(1 - \phi)\nabla p + \frac{\mu(1 - \phi)^2}{k}(\mathbf{v} - \mathbf{w}) = 0, \quad (4)$$

101 where μ is the water viscosity, k is the grain permeability. By analogy with (4), the momen-
102 tum equation for the polymer takes the form

$$-\phi\nabla p_s - \frac{\mu(1 - \phi)^2}{k}(\mathbf{v} - \mathbf{w}) = 0, \quad (5)$$

103 where p_s [Pa], is the pressure of the polymer. Note that our approach in dropping the
104 viscous stress for equations (8) and (9) is consistent with the the work of [Winstanley et al](#)
105 (2011), where the viscous stress was observed to be negligible compared to osmotic stress
106 and pressure. The interaction pressure, which is the pressure difference between the polymer
107 pressure and the water pressure, is given by

$$p_s - p = \psi(\phi).$$

108 Note that, a polymer in contact with water will swell (or shrink) to equilibrate the total
109 osmotic pressure - and swelling (in the current context) will give rise to changes in ϕ . It has
110 been recognised that the balance equations can be generalized to have a proper coupling to
111 thermodynamics, so that they have the correct driving forces for the transport phenomena
112 ([van der Sman, 2012](#)). Keeping this in mind, as will be shown next, here we adopt the
113 Flory-Huggins theory to relate the osmotic pressure to the polymer volume fraction, i.e.,
114 $\psi = \psi(\phi)$. At this point it may be noted that the processes of diffusion and diffusivity are
115 fundamentally different in nature, although they are formally described by the same type of
116 mathematics.

117 We now manifest the Flory-Huggins free energy per unit volume, as the osmotic pressure
118 term (see c.f. [Hill \(1987\)](#)), which is the additional pressure that is required to equilibrate
119 the solid (polymer) volume fraction with pure water. This is given by-

$$\psi = -\frac{RT}{V} \left[\ln(1 - \phi) + \left(1 - \frac{1}{n}\right) \phi + \chi \phi^2 \right] \quad (6)$$

120 where n is the ratio of molar volumes of solute (protein) and solvent (water), χ is the
121 interaction parameter between the polymer and the solvent (water), R [$\text{J mol}^{-1} \text{K}^{-1}$] is the
122 gas constant, T [K] is the temperature and V [$\text{m}^3 \text{mol}^{-1}$] is the molar volume of water.
123 The underpinning principles of the theory are backed up by strong thermodynamic basis
124 and the lattice theory, a good discussion of which can be found in [Hill \(1987\)](#). From a
125 thermodynamic viewpoint, the parameter χ is a measure of the interaction enthalpy per
126 solvent (water) molecule. Proceeding further, if n is sufficiently large ($n \rightarrow \infty$), which is
127 a valid assumption for the case of most foods, including navy bean, equation (6) can be

128 simplified to

$$\psi = -\frac{RT}{V} [\ln(1 - \phi) + \phi + \chi\phi^2]. \quad (7)$$

129 3.1. Model summary

Assuming incompressibility, we summarize the equations as follows

$$-f\phi(1 - \phi)(\mathbf{v} - \mathbf{w}) - \phi\nabla\psi - \phi\nabla p = 0, \quad (8)$$

$$f\phi(1 - \phi)(\mathbf{v} - \mathbf{w}) - (1 - \phi)\nabla p = 0, \quad (9)$$

$$\phi_t + \nabla \cdot [\phi\mathbf{v}] = 0, \quad (10)$$

$$-\phi_t + \nabla \cdot [(1 - \phi)\mathbf{w}] = 0, \quad (11)$$

$$\psi = -\frac{RT}{V} [\ln(1 - \phi) + \phi + \chi\phi^2], \quad (12)$$

130 where $f = \frac{\mu(1 - \phi)}{k\phi}$ [Pa s m⁻²] is the interfacial drag term. The model above incor-
 131 porates the momentum balance (Darcy's law) for each phase (equations (8) and (9)), the
 132 osmotic pressure equation (Flory-Huggins equation (12)) relating the chemical potential of
 133 the solvent (water) the solute (polymer), and mass conservation for each phase (equations
 134 (10) and (11)).

135 The swelling/shrinking pressure is proportional to $-\nabla\psi = -\psi'(\phi)\nabla\phi$ where

$$\psi'(\phi) = \frac{RT}{V} \frac{2\phi^2}{1 - \phi} \left[\left(\chi - \frac{1}{2} \right) - \chi\phi \right].$$

136 Here we consider $\psi' > 0$ where a polymer in contact with a solvent will swell. We note that
 137 for $\phi \in [0, 1]$, there is a minimum at $\phi^* = (\chi - \frac{1}{2})/\chi$ with $\chi > \frac{1}{2}$, as can be observed in Fig.
 138 2. The above relation can therefore be used for tracking the equilibrium moisture interface
 139 over a moving boundary.

After some algebraic simplification, the system of equations (8) – (12) can be reduced to

$$\phi_t = \nabla \cdot [(1 - \phi)\mathbf{w}], \quad (13)$$

$$\mathbf{w} = \frac{\phi}{f(\phi)} \psi'(\phi) \nabla \phi, \quad (14)$$

$$\psi = -\frac{RT}{V} [\ln(1 - \phi) + \phi + \chi\phi^2]. \quad (15)$$

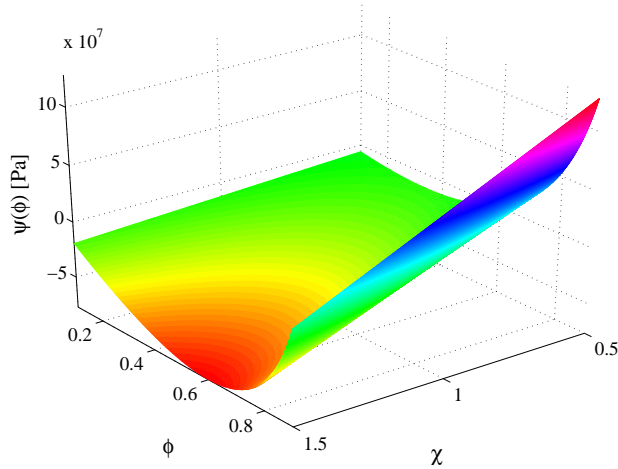


Figure 2: An illustration of the relationship between osmotic pressure and polymer fraction.

140 Assuming one dimensional spherical coordinate system, then $\phi(r, t)$ is shown to be gov-
 141 erned by the Fick's second Law of diffusion

$$\frac{\partial \phi}{\partial t} = \frac{1}{r^2} \frac{\partial}{\partial r} \left[r^2 D(\phi) \frac{\partial \phi}{\partial r} \right], \quad (16)$$

142 where the moisture diffusivity term is given by

$$D(\phi) = D_0 \frac{2\phi^3}{1-\phi} \left[\chi\phi - \left(\chi - \frac{1}{2} \right) \right], \quad (17)$$

143 and $D_0 = \frac{RTk}{\mu V}$. We now require that $\chi\phi - (\chi - \frac{1}{2}) > 0$ or $\phi^* < \phi < \phi_e$. The Flory's
 144 interaction parameter, χ in this range corresponds to approx. [0.5-1.5], which also complies
 145 with the values reported in [Jin et al \(2014\)](#). This will be used later to motivate the choice
 146 of boundary condition at the interface between free water and the porous structure. This
 147 constrain also arises from the peculiar nature of χ as the parameter dictating the phase
 148 separations in polymer-solvent systems, a comment on which is appropriate. The critical
 149 value of χ (denoted as χ_c) for miscibility of a polymer in a solvent is approximately 0.5. For
 150 values of χ less than 0.5 the polymer will be soluble in the solvent and loss of solids (leaching)
 151 will occur. However, the analogous polymer-solvent theory for navy bean assuming no loss
 152 of solids (solute) requires that the biopolymer matrix be insoluble in the water, i.e. a poor
 153 solvent behaviour. Therefore, our assumption of $\chi > \frac{1}{2}$ is physically valid, for only with this
 154 constrain the polymer will not be soluble in the solvent ([Flory, 1953](#); [Hill, 1987](#)).

155 It is worth noting the similarities between the derived model and the literature; see for ex-
156 ample [Bello et al \(2010\)](#); [Davey et al \(2002\)](#); [Weinstein and Bennethum \(2006\)](#); [Nicolin et al](#)
157 [\(2012\)](#). In particular, [Davey et al \(2002\)](#) derived a nonlinear diffusion equation governing
158 the swelling of a cereal grain. However, the model here deviates from [Davey et al \(2002\)](#)
159 in the choice of the diffusivity function. While their choice is motivated by an empirical
160 exponential function, here the function comes naturally from the Flory-Huggins theory. A
161 model based on thermodynamics arguments and Flory-Huggins theory was also presented
162 by [Weinstein and Bennethum \(2006\)](#). The resulting nonlinear diffusion equation can be re-
163 duced to the model derived here with the condition that $\chi = 0$ and an appropriate choice of
164 the permeability function. However, as we have observed earlier, the limit $\chi = 0$ does not
165 make any physical sense.

166 From a mathematical point of view, the presented model is a moving boundary problem
167 and requires an extra condition for the location of the boundary $r = R(t)$. As the water
168 is absorbed, the grain swells and there is a change of mass inside the grain. From here
169 forthwith, we define $\phi = 1 - \theta$, so that θ defines the volume fraction of water and $1 - \theta$ the
170 volume fraction of the polymer. Using the new variable we have

$$\frac{\partial \theta}{\partial t} = \frac{1}{r^2} \frac{\partial}{\partial r} \left[r^2 D(\theta) \frac{\partial \theta}{\partial r} \right], \quad (18)$$

171

$$D(\theta) = D_0 \frac{2(1 - \theta)^3}{\theta} \left[\chi(1 - \theta) - \left(\chi - \frac{1}{2} \right) \right], \quad (19)$$

172 with $\theta > 0$. Integrating (18) on $r \in [0, R(t)]$ and on application of Leibniz rule, we have

$$R^2 \frac{dR}{dt} = \frac{D(\theta_e) R^2}{1 - \theta_e} \frac{\partial \theta}{\partial r} \Big|_{r=R(t)} + \frac{1}{1 - \theta_e} \frac{d}{dt} \left[\int_0^{R(t)} (1 - \theta) r^2 dr \right], \quad (20)$$

173 where we have used symmetry and the fact that $\theta_r = 0$ on $r = 0$. The middle term gives
174 the flux of water through the grain and the last term gives the dissolution rate. Here there
175 is no loss of solid during hydration, hence we set

$$\frac{d}{dt} \left[\int_0^{R(t)} (1 - \theta) r^2 dr \right] = 0, \quad (21)$$

176 so that the moving boundary is described by

$$\frac{dR}{dt} = \frac{D(\theta_e)}{1 - \theta_e} \frac{\partial \theta}{\partial r} \Big|_{r=R(t)}. \quad (22)$$

177 3.2. Boundary Conditions

As initial condition, we know that $\theta(r, 0) = \theta_0$ under the assumption that the moisture distribution inside the bean is isotropic. We now specify the boundary conditions as follows

$$\frac{\partial \theta}{\partial r} = 0, \quad \text{on } r = 0, \quad (23)$$

$$\theta = \theta_e, \quad \text{on } r = R(t). \quad (24)$$

178 The volume averaged moisture content at each time step, t [s] is calculated from equation
179 (25), as given by Ruiz et al (2008),

$$M(t) = \frac{3}{R(t)^3} \int_0^{R(t)} R(t)^2 \theta(R, t) dr, \quad (25)$$

180 where $R(t)$ is the radius at time t [s]. For validation of the model, we employ the experimental
181 results from a previous work Ghafoor et al (2014) and set all parameters as per Table 1,
182 unless otherwise explicitly stated. The moisture content on dry basis given in Ghafoor et al
183 (2014) was transformed into volume fraction of water, $\theta(r, t)$, using the following relation

$$M = \frac{\rho \theta}{\rho_s (1 - \theta)}, \quad (26)$$

184 where, as defined before, ρ and ρ_s are the density of water and the solid respectively.

185 4. Nondimensionalisation

186 We introduce the following scales

$$r \sim \ell, \quad s \sim \ell, \quad R \sim \ell, \quad D \sim D_0, \quad t \sim \frac{\ell^2}{D_0}, \quad (27)$$

where ℓ is the initial bean radius. The advantage of this process is that we now have to solve the model on $[0, R(t)]$ with $R(t) \geq 1$. In dimensionless form, we consider

$$\frac{\partial \theta}{\partial t} = \frac{1}{r^2} \frac{\partial}{\partial r} \left[r^2 D(\theta) \frac{\partial \theta}{\partial r} \right], \quad \forall (r, t) \in (0, R(t)) \times (0, \infty), \quad (28)$$

$$\theta(r, 0) = \theta_0, \quad (29)$$

Table 1: Typical values of the parameters employed for the simulations and model validation.

Symbol	Definition	Value		Source
θ_0	Initial water fraction	0.12		Ghafoor et al (2014)
θ_e	Equilibrium water fraction	0.60		Ghafoor et al (2014)
T	Temperature	289.15	K	Ghafoor et al (2014)
ℓ	Navy bean initial radius	0.003	m	Ghafoor et al (2014)
ρ_s	Polymer matrix density	1376	kg/m ³	Bellido et al (2003)
ρ	Density of water	999.1	kg/m ³	
μ	Viscosity of water	1.109×10^{-3}	Pa s	
k	Permeability	3.1×10^{-21} (approx.)	m ²	Warning et al (2014)
χ	Interaction parameter	0.51		Jin et al (2014)
R	Gas constant	8.314	J/mol/K	
V	Molar volume of water	18.02×10^{-6}	m ³ /mol	
D_0	$RTk/\mu V$	4.81×10^{-10}	m ² /s	

subject to

$$\frac{\partial \theta}{\partial r}(0, t) = 0, \quad (30)$$

$$\theta(R, t) = \theta_e, \quad \text{and} \quad \frac{dR}{dt} = \frac{D(\theta_e)}{1 - \theta_e} \frac{\partial \theta}{\partial r} \Big|_{r=R(t)}, \quad (31)$$

187 where

$$D(\theta) = \frac{2(1 - \theta)^3}{\theta} \left[\chi(1 - \theta) - \left(\chi - \frac{1}{2} \right) \right]. \quad (32)$$

188 While some mathematical insight can be obtained from an equivalent two moving boundary
189 problem as in Davey et al (2002), here no analytical approximation is possible. Hence we
190 proceed to solve the problem numerically.

191 **5. Numerical simulations and model validation**

192 The model is discretized in space using finite volume approach on the domain $[0, R(t)]$
 193 with N uniform grid cells of width $\Delta r = R(t)/N$ with cell centers $r_{i\pm\frac{1}{2}} = r_i \pm \frac{\Delta r}{2}$ for
 194 $i = 1, 2, \dots, N$. Using the notation consistent with the finite volume literature, we have the
 195 scheme

$$\frac{\partial\theta_i}{\partial t} = \frac{1}{r_i^2\Delta r} \left[r_{i+1/2}^2 D_{i+1/2} \frac{\theta_{i+1} - \theta_i}{\Delta r} - r_{i-1/2}^2 D_{i-1/2} \frac{\theta_i - \theta_{i-1}}{\Delta r} \right]. \quad (33)$$

196 for equation (28), and

$$\frac{dR}{dt} = \frac{D(\theta_e)}{1 - \theta_e} \frac{\theta_{i+1/2} - \theta_{i-1/2}}{\Delta r} \Big|_{r_i=R(t)} \quad (34)$$

197 for the moving boundary (31). The same approach is used for the boundary conditions
 198 and the resulting scheme is second order in space. The solution code scripted in MATLAB
 199 (The MathWorks, MA, USA) was run on a 3.0 GHz Intel Core i7 processor. The system of
 200 nonlinear ODEs are integrated with Matlab's standard stiff solver ODE15s, with a relative
 201 tolerance values of 1×10^{-12} . The resolution algorithm of ODE15s is based on the numerical
 202 differentiation formula method (improved version of the implicit Backward Differentiation
 203 Formula (BDF) method). For all the simulations presented in this paper, we used $N = 201$
 204 and we found no influence on the results upon rerunning the simulations with increased
 205 number of nodes.

206 For evaluating the accuracy of the models, we employ the statistical criterion of the Root
 207 Mean Squared Error (RMSE) given by equation (35)

$$RMSE = \sqrt{\frac{\sum_{i=1}^{n_t} (\theta_e - \theta_p)^2}{n_t}} \quad (35)$$

208 where θ_e denotes the experimental observations, θ_p the predicted values and n_t the total
 209 number of data points.

210 *5.1. Base case simulations*

211 We now compare our results with the experimental data reported by [Ghafoor et al \(2014\)](#),
 212 who studied the hydration of navy beans in water at 16 °C. Figure 3 (a) provides a compari-
 213 son of the model predictions and the experimental data. The model clearly provides a good

214 prediction of the hydration kinetics, within a reasonably small error as observed from the
 215 RMSE value of 0.081. At the beginning of the water absorption process, the relative mass
 216 of water absorbed by the bean cotyledon strongly increased with the hydration time and
 217 then saturated. The exponential behaviour indicates that the water absorption is caused
 218 by the gradient of the matrix potential between the dry cotyledon structure and the wa-
 219 ter environment (Golonka et al, 2002). The volume fraction of the liquid representing the
 220 moisture content tends to approximately a value of 0.6 after 15 h of soaking. In addition,
 221 we note that the radius of the representative bean follows a similar trend and swells to a
 222 maximum radii of ~ 3.9 mm, which is in excellent agreement with the experimental value
 223 of 3.92 mm. We wish to highlight that unlike, the work of Bakalis et al (2009) and Hsu
 224 (1983) who employ experimental observations and empirical equations respectively for the
 225 bean swelling, our approach accurately predicts the radii as a function of the instantaneous
 226 moisture. The deviation from the experimental values during the initial phase of hydra-
 227 tion can be ascribed to our ignorance of resistance offered by the seed coat. This fact is
 228 experimentally demonstrated elsewhere in the context of soybean hydration (Meyer et al,
 229 2006).

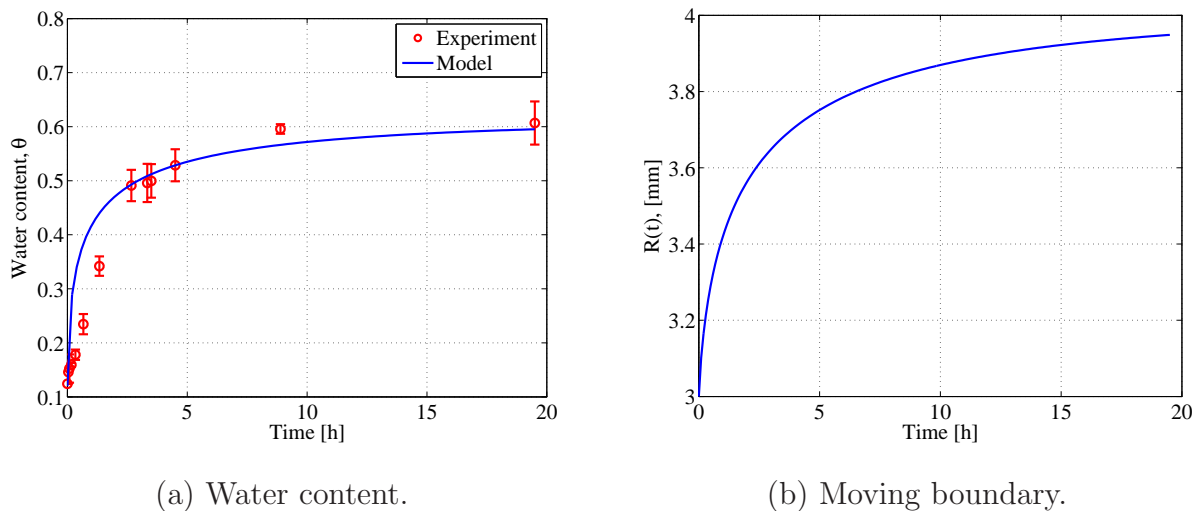


Figure 3: Profiles for water content and the radius of the bean with time.

230 5.2. Degree of hydration

231 An earlier work on cooking of grains focused on the degree of gelatinisation of a rice
232 kernel and the significant feature of this model was the presence of two moving boundaries.
233 One describing the change in grain size and the second boundary described the gelatinisation
234 front (Davey et al, 2002). Mathematically, these represent a class of Stefan’s problem where
235 no phase change is involved (see, for example Barry and Counce (2008)). Since cooking
236 temperatures leading to gelatinisation are never encountered for simple hydration, we are left
237 with one moving boundary for the radius and a transient species diffusion. Equivalently, here
238 we implicitly locate the degree of hydration by tracking the front where the moisture content
239 is θ_w . This approach is more physically representative since we are effectively allowing
240 moisture variations beyond the wetting front. We present these relations via. a contour
241 plot in Figure 4. The rapid hydration in the initial phase can be ascribed to the creation of
242 free volumes inside the grains, while the slow water uptake in later phases is an outcome of
243 the rearrangement of structural elements. Direct experimental observations using Positron
244 Annihilation Spectroscopy (PAS) and proton Nuclear Magnetic Relaxation (NMR) reported
245 earlier also support our hypothesis and explanation (Golonka et al, 2002). Golonka et al
246 (2002) reported that the hydration of the cotyledon structure evokes reduction of the surface
247 and interior tension, and loosens structure of the bean samples. When the hydration reaches
248 the slower phase, a rearrangement of the cotyledon microstructure occurs and the number
249 and dimensions of the free volume regions does not change significantly.

250 5.3. Sensitivity to bean dimensions

251 Experimental measurement of the initial bean dimensions of several beans and the av-
252 erage values a , b and c were in the range 8.9 ± 0.39 mm, 5.04 ± 0.15 mm and 5.9 ± 0.28 mm
253 respectively, see Ghafoor et al (2014). The bean dimensions after a 19 h soaking duration
254 were found to be in the range 12.94 ± 0.47 mm, 6.32 ± 0.31 mm and 7.54 ± 0.21 mm respec-
255 tively. These values corresponded to an initial and final radii of the equivalent sphere in
256 the range 3 mm and 4 mm respectively. Differences in bean dimensions affect the degree
257 of hydration, especially for shorter hydration times, which nevertheless, is overcome with

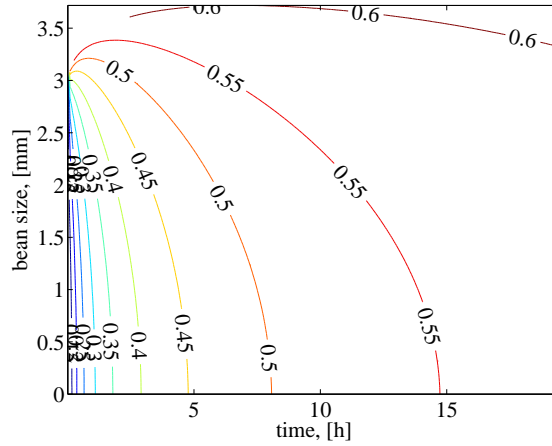
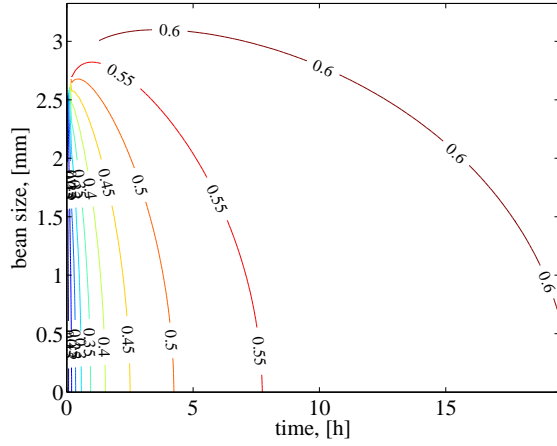


Figure 4: The isolines represent the degree of hydration of the grain at a given time.

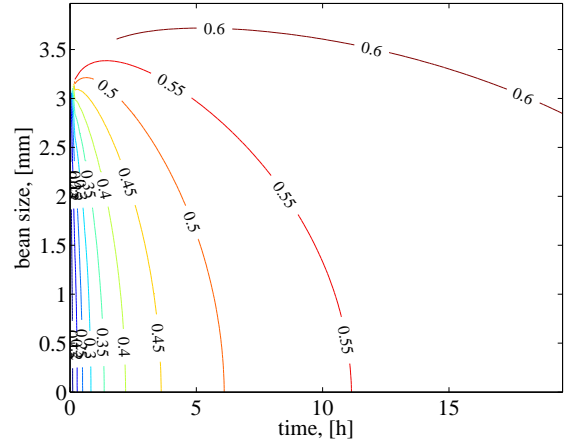
258 standard overnight soaking practice. We performed sensitivity analysis for the degree of
 259 hydration to bean dimensions in the range 2.5 to 4.0 mm. The results are summarised in
 260 Figure 5. Firstly, we note that beans with higher initial radii swell to higher degree and
 261 this was also observed during the experiments (Ghafoor et al, 2014). Next, the moisture
 262 equilibration takes more time for larger beans. However, longer soaking times allow to reach
 263 near equilibrium moisture distribution.

264 5.4. Sensitivity to medium permeability

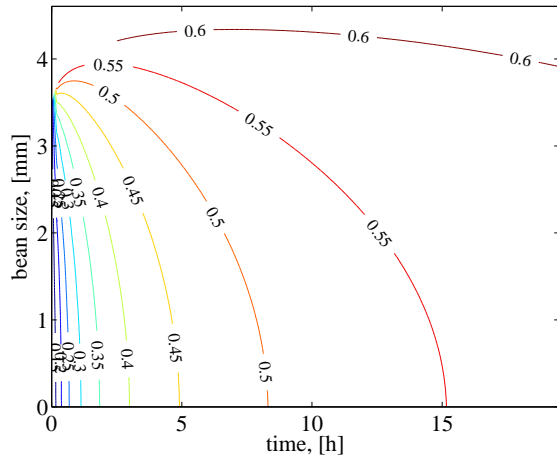
265 When considering the moisture diffusion in a single bean, the porosity, pore network
 266 size and distribution largely define the rate of hydration. Since we chose porosity as a
 267 macroscopic variable in our model, the above factors are ruled by the intrinsic permeability
 268 in this framework. Datta (2006) highlighted that when physics based mechanistic models
 269 involving pressure driven flow are employed with a clear definition of the individual modes of
 270 transport processes, the selection of permeability data becomes important. Considering that
 271 we did not find experimentally measured permeability data for navy beans, we approximated
 272 the intrinsic permeability from that of parboiled rice grains and those reported for other inert
 273 materials (Warning et al, 2014; Datta, 2006). The permeability for heat treated parboiled
 274 rice grain was recently reported to be in the order of 10^{-20} m² using Lattice-Boltzmann
 275 simulations. As rice grain hydrates to more than double its volume whereas navy bean to



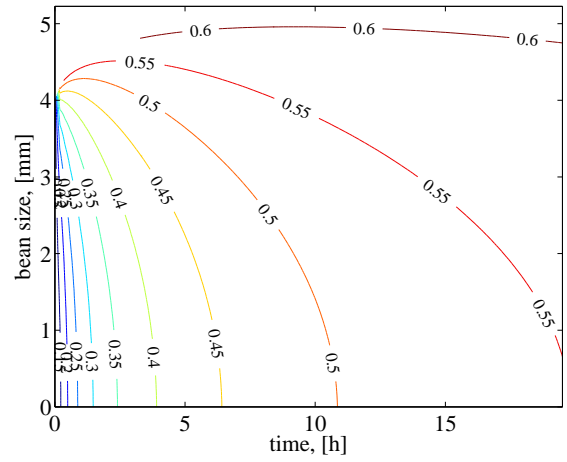
(a) Initial radius 0.0025 mm.



(b) Initial radius 0.003 mm.



(c) Initial radius 0.0035 mm.



(d) Initial radius 0.004 mm.

Figure 5: Profiles for the bean radius for different initial bean radii taken in the range [2.5 – 4.0] mm.

276 approximately 1.2 times the original volume, we take values in the order of 10^{-21} m^2 . To
 277 gauge the sensitivity of the model to permeability value we performed sensitivity analysis
 278 in the range $[1.1 - 5.1] \times 10^{-21} \text{ m}^2$. The sensitivity of the moisture content of the bean
 279 is presented in Figure 6. It can be observed that the evolution of water saturated pore
 280 fraction is directly related to the intrinsic permeability. This indicates the strong coupling
 281 between the momentum transport and structure evolution in our model. The model was
 282 thus found to be highly sensitive to the selection of permeability values, where a higher
 283 permeability indicated a faster rate of hydration. It is worth noting that a non-linearly
 284 evolving permeability will allow far more accurate predictions than a constant value. This

285 is true considering that the porosity of the bean evolves with time. A direct method for
 286 applying the model could be based on the microstructure geometry, similar to that described
 287 by Nicolaí and group in their recent work using micro- computed tomography method for
 288 fruits (Cantre et al, 2014; Herremans et al, 2014). Conversely, our analysis can also be
 289 transformed to an inverse problem scenario to compute the effective water permeability.

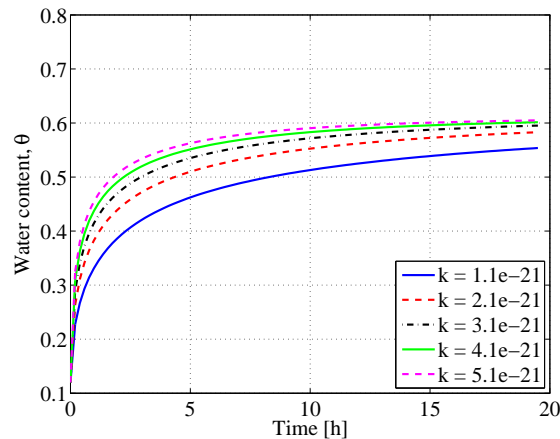


Figure 6: Profiles for the water content for different permeability values taken in the range $[1.1 - 5.1] \times 10^{-21}$ m^2 .

290 6. Conclusions

291 The SCM model demonstrated good predictive capabilities for moisture transport and
 292 swelling of the navy beans, without losing the elegance of internal porodynamics. The
 293 moving boundary equation accurately predicted the final radii of the bean and supported
 294 the rapid creation of free volume inside the bean during rapid hydration phase, followed
 295 by structural rearrangements observed in experiments. The model was found sensitive to
 296 the selection of the permeability value and modelling on accurate physical domain is highly
 297 encouraged. The model presented here is a proof of concept of how hydration of foods can
 298 be described by using principles of soft condensed matter physics.

299 To impart an illustrative value, we simplified the model with some assumptions, so that
 300 the theory could be easily discussed. Although we demonstrated the applicability of the
 301 model with spherical equivalence and radial profile simulations, the extension of this model

302 to foods with complex geometry should be quite straightforward, using finite volume or
303 finite element methods with moving mesh or phase-field and level set approaches using
304 commercial softwares such as COMSOL Multiphysics. This is now practical since significant
305 microstructural details are becoming available with newer imaging techniques such as X-ray
306 micro-computed tomography. The model can be elaborated for cooking of food grains by
307 incorporating the Fourier equation. As a limitation of the current single grain modeling
308 approach, we wish to highlight that diffusion in a single particle is different physically from
309 diffusion through a porous particle layer. Thus, to simulate realistic conditions, the problem
310 turns out to be a two-phase, multiscale, saturated porous media problem. This will be dealt
311 with in our future work.

312 References

- 313 Abd El-Hady E, Habiba R (2003) Effect of soaking and extrusion conditions on antinutrients and protein di-
314 gestibility of legume seeds. *LWT - Food Science and Technology* 36:285–293, DOI 10.1016/s0023-6438(02)
315 00217-7
- 316 Bakalis S, Kyritsi A, Karathanos VT, Yanniotis S (2009) Modeling of rice hydration using finite elements.
317 *Journal of Food Engineering* 94:321 – 325, DOI 10.1016/j.jfoodeng.2009.03.023
- 318 Barry SI, Caunce J (2008) Exact and numerical solutions to a stefan problem with two moving boundaries.
319 *Applied Mathematical Modelling* 32:83–98, DOI 10.1016/j.apm.2006.11.004
- 320 Bellido G, Arntfield S, Scanlon M, Cenkowski S (2003) The effect of micronization operational conditions on
321 the physicochemical properties of navy beans (*Phaseolus vulgaris* L.). *Journal of Food Science* 68:1731–
322 1735, DOI 10.1111/j.1365-2621.2003.tb12320.x
- 323 Bello M, Tolaba M, Aguerre R, Suarez C (2010) Modeling water uptake in a cereal grain during soaking.
324 *Journal of Food Engineering* 97:95–100, DOI 10.1016/j.jfoodeng.2009.09.020
- 325 Berg T, Singh J, Hardacre A, Boland MJ (2012) The role of cotyledon cell structure during in vitro digestion
326 of starch in navy beans. *Carbohydrate Polymers* 87:1678 – 1688, DOI 10.1016/j.carbpol.2011.09.075
- 327 Cantre D, East A, Verboven P, Trejo Araya X, Herremans E, Nicolaí BM, Pranamornkith T, Loh M, Mowat
328 A, Heyes J (2014) Microstructural characterisation of commercial kiwifruit cultivars using x-ray micro
329 computed tomography. *Postharvest Biology and Technology* 92:79–86, DOI 10.1016/j.postharvbio.2014.
330 01.012
- 331 Cozzolino D, Roumeliotis S, Eglinton J (2013) Monitoring water uptake in whole barley (*Hordeum vulgare* L.)

332 grain during steeping using near infrared reflectance spectroscopy. *Journal of Food Engineering* 114:545–
333 549, DOI 10.1016/j.jfoodeng.2012.09.010

334 Datta A (2006) Hydraulic permeability of food tissues. *International Journal of Food Properties* 9:767–780,
335 DOI 10.1080/10942910600596167

336 Davey M, Landman K, McGuinness M, Jin H (2002) Mathematical modeling of rice cooking and dissolution
337 in beer production. *AIChE Journal* 48(8):1811–1826

338 Flory PJ (1953) *Principles of Polymer Chemistry*. Cornell University Press

339 Ghafoor M, Misra N, Mahadevan K, Tiwari B (2014) Ultrasound assisted hydration of navy beans (*Phaseolus*
340 *vulgaris*). *Ultrasonics Sonochemistry* 21:409–414, DOI 10.1016/j.ultsonch.2013.05.016

341 Golonka P, Dryzek J, Kluza M (2002) Bean cotyledons microporosity under hydration conditions. *Nukleonika*
342 47:137–140

343 Hamley IW (2007) *Polymers*, Wiley, chap 2, pp 39–106

344 Han CC, Akcasu ZA (2011) *Dynamics and Kinetics of Phase Separation in Polymer Systems*, John Wiley
345 & Sons, chap 3, pp 103–209. DOI 10.1002/9780470824849.ch3

346 Herremans E, Verboven P, Defraeye T, Rogge S, Ho QT, Hertog ML, Verlinden BE, Bongaers E, Wevers M,
347 Nicolai BM (2014) X-ray CT for quantitative food microstructure engineering: The apple case. *Nuclear*
348 *Instruments and Methods in Physics Research Section B: Beam Interactions with Materials and Atoms*
349 324:88–94, DOI 10.1016/j.nimb.2013.07.035

350 Hill TL (1987) *Polymer and polyelectrolyte solutions and gels*, Dover Publications, chap 21, pp 398–423

351 Hsu KH (1983) A diffusion model with a concentration-dependent diffusion coefficient for describing water
352 movement in legumes during soaking. *Journal of Food Science* 48:618–622, DOI 10.1111/j.1365-2621.1983.
353 tb10803.x

354 Huggins ML (1942a) Some properties of solutions of long-chain compounds. *The Journal of Physical Chem-*
355 *istry* 46:151–158, DOI 10.1021/j150415a018

356 Huggins ML (1942b) Theory of solutions of high polymers. *Journal of the American Chemical Society*
357 64:1712–1719, DOI 10.1021/ja01259a068

358 Jin X, van der Sman RGM, Maanen JFC, Deventer HC, Straten G, Boom RM, Boxtel AJB (2014) Moisture
359 sorption isotherms of broccoli interpreted with the flory-huggins free volume theory. *Food Biophysics*
360 9:1–9, DOI 10.1007/s11483-013-9311-6

361 Kereliuk G, Kozub G (1995) Chemical composition of small white (navy) beans. *LWT - Food Science and*
362 *Technology* 28:272–278, DOI 10.1016/s0023-6438(95)94176-2

363 Meyer CJ, Steudle E, Peterson CA (2006) Patterns and kinetics of water uptake by soybean seeds. *Journal*
364 *of Experimental Botany* 58:717–732, DOI 10.1093/jxb/erl244

365 Mezzenga R (2007) Equilibrium and non-equilibrium structures in complex food systems. *Food Hydrocolloids*

21:674–682, DOI 10.1016/j.foodhyd.2006.08.019

Mezzenga R, Schurtenberger P, Burbidge A, Michel M (2005) Understanding foods as soft materials. *Nature Materials* 4:729–740, DOI 10.1038/nmat1496

Mohoric A, Vergeldt F, Gerkema E, de Jager A, van Duynhoven J, van Dalen G, Van As H (2004) Magnetic resonance imaging of single rice kernels during cooking. *Journal of Magnetic Resonance* 171:157–162, DOI 10.1016/j.jmr.2004.08.013

Mohsenin NN (1986) *Physical Properties of Plant and Animal Materials*. Routledge

Nicolin D, Coutinho M, Andrade CM, Jorge L (2012) Hsu model analysis considering grain volume variation during soybean hydration. *Journal of Food Engineering* 111:496–504, DOI 10.1016/j.jfoodeng.2012.02.035

Peleg M (1988) An empirical model for the description of moisture sorption curves. *Journal of Food Science* 53:1216–1217, DOI 10.1111/j.1365-2621.1988.tb13565.x

Ruiz RS, Vizcarra MG, Martínez C (2008) Hydration of grain kernels and its effect on drying. *LWT - Food Science and Technology* 41:1310–1316, DOI 10.1016/j.lwt.2007.08.007

van der Sman R (2012) Soft matter approaches to food structuring. *Advances in Colloid and Interface Science* 176-177:18–30, DOI 10.1016/j.cis.2012.04.002

van der Sman RGM (2007) Soft condensed matter perspective on moisture transport in cooking meat. *AIChE Journal* 53:2986–2995, DOI 10.1002/aic.11323

van der Sman RGM, van der Goot AJ (2009) The science of food structuring. *Soft Matter* 5:501, DOI 10.1039/b718952b

Ubbink J, Mezzenga R (2006) Delivery of functionality in complex food systems: introduction. *Trends in Food Science & Technology* 17:194–195, DOI 10.1016/j.tifs.2006.01.004

Ubbink J, Burbidge A, Mezzenga R (2008) Food structure and functionality: a soft matter perspective. *Soft Matter* 4:1569, DOI 10.1039/b802183j

Wang H, Swain E, Hesseltine C, Heath H (1979) Hydration of whole soybeans affects solid losses and cooking quality. *Journal of Food Science* 44:1510–1513, DOI 10.1111/j.1365-2621.1979.tb06474.x

Warning A, Verboven P, Nicolaí B, van Dalen G, Datta AK (2014) Computation of mass transport properties of apple and rice from x-ray microtomography images. *Innovative Food Science & Emerging Technologies* pp in–press, DOI 10.1016/j.ifset.2013.12.017

Weinstein T, Bennethum L (2006) On the derivation of the transport equation for swelling porous materials with finite deformation. *International Journal of Engineering Science* 44(18):1408–1422

Winstanley H, Chapwanya M, McGuinness M, Fowler A (2011) A polymer-solvent model of biofilm growth. *Proceedings of the Royal Society A: Mathematical, Physical and Engineering Science* 467(2129):1449–1467

Zanella-Díaz E, Mújica-Paz H, Soto-Caballero M, Welti-Chanes J, Valdez-Fragoso A (2014) Quick hydration of tepary (phaseolus acutifolius a. gray) and pinto beans (*Phaseolus vulgaris* L.) driven by pressure

